25th ABCM International Congress of Mechanical Engineering
October 20-25, 2019, Uberlândia, MG, Brazil

COBEM2019-0829
WIND-INDUCED VIBRATIONS SIMULATION OF BEAM-LIKE STRUCTURES

Weber Alves Braga
Mechanical Engineering Postgraduate Program, Federal University of Uberlândia, Av. João Naves de Ávila, 2121, CEP: 38400-902, Uberlândia, MG, Brazil
weberfila15@gmail.com

Francisco da Silva Brandão
Civil Engineering Postgraduate Program, Federal University of Rio Grande do Sul, Av. Osvaldo Aranha, 99, CEP 90035-190, Porto Alegre, RS, Brazil
eng.fsbrandao@gmail.com

Juscelino Chaves Sales
Department of Civil Engineering, State University of Vale do Acaraú, Av. Dr. Guarany, 317, CEP 62040-730, Sobral, CE, Brazil
juscelinochaves@hotmail.com

Abstract. *This paper presents the simulation of the dynamic response of a slender building of 60 meter high submitted to wind. From theory of bridge aerodynamics this study was developed and to apply the theory for a tower structure, some small changes and assumptions has been made. To determine basic dynamic properties for the given structure, a modal analysis was conducted using SAP2000 software. A MATLAB script was made to perform all calculations using given and estimated input values to fit accelerations calculations for the two first translational modes. The script carried out time domain simulation for a single mode excitation of the structure by the previous calculation of their spectral densities.*

Keywords: *structural dynamics, buffeting response, time domain simulation.*

1. INTRODUCTION

The influence of wind on structures is a complex subject. The wind field varies both in space and time, and thus a statistical approach is demanded to describe wind loading. For low and stiff structures, wind induces surface pressure and suction, which could be critical for facades and roofs. In bridges and tall buildings, the effects of wind are more complicated. Wind acting on tall and slender structures could result in several effects, among them buffeting and vortex shedding. These effects induce vibrations in the structure, which could lead to major displacements, accelerations and resulting forces.

This paper is based on work of Braga (2018) and aimed to gain knowledge and understanding of the effects that turbulent wind has on tall buildings. From theory of bridge aerodynamics of Einar Strømmen (2010) the theoretical basis of this study was developed. To make the theory applicable to a tower structure, some small changes and assumptions has been made. To determine basic dynamic properties for the given structure, a modal analysis was conducted using SAP2000 software. A MATLAB script was made to perform all calculations using given and estimated input values to fit accelerations for the two first translational modes of a benchmark tall building.

The book *Theory of Bridge Aerodynamics* of Einar Strømmen (2010) contains all the theory needed to investigate the wind induced response of structures. Theory of Bridge Aerodynamics is formulated for horizontal, line like bridges, but all considerations are feasible to fit calculations for any horizontal beam-like structure. To make it, some small changes and assumptions has been made and one of the most important ones is how a structure is considered. For bridges, the main wind flow acts on one side of the bridge deck cross section. For a tower structure, however, the main flow could come from any direction. The maximal response from a single mode excitation will occur when the main flow acts in the same direction as the modal displacement. As a result of the above, main flow has been assumed to act in the same direction as the modal displacements for all modes.

2. BUFFETING RESPONSE

The derivation that follows covers single mode, single component response calculations. It is presupposed that eigen frequencies are well separated and that coupling effects are negligible. As mentioned earlier, only one modal shape is included in the calculation at a time, and the resulting response has one component.

2.1 Spectral Density of Displacement

In buffeting response analysis, the standard deviation of displacement is given by integrating the spectral density of displacement over the entire frequency domain. To obtain the spectral density of displacement, it is convenient to start with the equation of motion on modal form, given by:

$$\tilde{M}_i \cdot \ddot{\eta}_i(t) + \tilde{C}_i \cdot \dot{\eta}_i(t) + \tilde{K}_i \cdot \eta_i(t) = \tilde{Q}_i(t) + \tilde{Q}_{ae_i}(\mathrm{t}, \eta, \dot{\eta}, \ddot{\eta}) \tag{1}$$

Here, M_i is the modal mass, C_i is the modal damping, and K_i is the modal stiffness for mode *i*. $\dot{\eta}$ e $\ddot{\eta}$ are the general coordinates derived by time. $\tilde{Q}_i(t)$ represents the flow induced loading on the structure, while $\tilde{Q}_{ae_i}(\mathrm{t}, \eta, \dot{\eta}, \ddot{\eta})$ represents the load given by interaction between structural motion and air flow. Applying the Fourier Transform, the following is obtained:

$$(\tilde{M}_i \omega^2 + \tilde{C}_i i\omega + \tilde{K}_i) \cdot a_{\eta_i} = a_{\tilde{Q}_i}(\omega) + a_{\tilde{Q}_{ae_i}}(\omega, \eta, \dot{\eta}, \ddot{\eta}) \tag{2}$$

The Fourier amplitude of the aerodynamic load term could be rewritten into a sum of cross sectional properties.

$$(\tilde{M}_{ae_i} \omega^2 + \tilde{C}_{ae_i} i\omega + \tilde{K}_{ae_i}) \cdot a_{\eta_i} = a_{\tilde{Q}_{ae_i}}(\omega) \tag{3}$$

Now using basic dynamic identities, inserting Eq. (2) into (3), moving $a_{\tilde{Q}_{ae_i}}$ to the left hand side, and dividing by $\tilde{K}_i = \omega_i^2 \tilde{M}_i$ it is obtained that:

$$\left(1 - \frac{\tilde{K}_{ae_i}}{\omega_i^2 \tilde{M}_i} - \left(1 - \frac{\tilde{M}_{ae_i}}{\tilde{M}_i}\right) \cdot \left(\frac{\omega}{\omega_i}\right)^2 + \left(\zeta_i - \frac{\tilde{C}_{ae_i}}{2\omega_i^2 \tilde{M}_i}\right) \frac{\omega}{\omega_i}\right) \cdot a_{\eta_i}(\omega) = \frac{a_{\tilde{Q}_i}(\omega)}{\tilde{K}_i} \tag{4}$$

Expression in Eq. (4) could be rewritten into the following expression:

$$a_{\eta_i}(\omega) = \frac{\hat{H}_i(\omega)}{\tilde{K}_i} \cdot a_{\tilde{Q}_i}(\omega) \tag{5}$$

$\hat{H}(\omega)$ contains all the aerodynamic cross-sectional properties. The spectral density of η is found by:

$$S_{\eta_i}(\omega) = \frac{\left|\hat{H}_i(\omega)\right|^2}{\tilde{K}_i^2} \cdot S_{\tilde{Q}_i}(\omega) \tag{6}$$

$S_{\tilde{Q}_i}(\omega)$ in Eq. (6) is the spectral density of loading. The spectral density of displacement, or response spectrum, is then given by:

$$S_{r_i}(\omega) = \frac{\phi_i^2(z_r)}{\tilde{K}_i^2} \left|\hat{H}_i(\omega)\right|^2 \cdot S_{\tilde{Q}_i}(\omega) \tag{7}$$

Strømmen (2010) shows how a discretization of a response spectrum could be used to perform a time domain simulation of response. A spectral density could be discretized by for each frequency interval *k*.

$$S_x(\omega_k) = \frac{c_k^2}{2\Delta\omega_k} \tag{8}$$

The amplitude parameter c_k could be obtained by:

$$c_k = (2 \cdot S_x(\omega_k) \cdot \Delta\omega_k) \tag{9}$$

The time series simulation is then given by:

$$x(t) = \sum_{k=1}^{N} c_k \cdot \cos(\omega_k t + \psi_k) \tag{10}$$

Where ψ_k is a random phase angel between 0 and 2π. Such a simulation will be performed both for displacement and acceleration when results are obtained.

2.2 Spectral Density of Loading

To determine an expression for the spectral density of loading, the expression for the load itself has to be established. The displacements and rotations of a cross-section due static and turbulence induced loading are shown in Fig. 1.

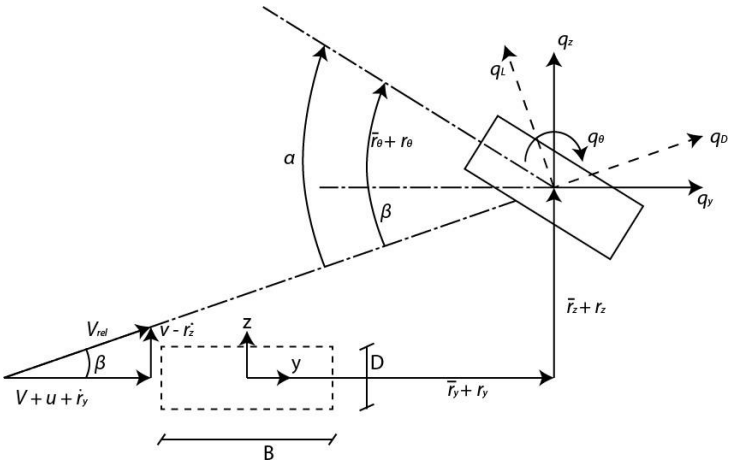

Figure 1. Force and displacements for wind loading.
Adapted from: Strømmen (2010)

The *x*-coordinate is defined as the height axis of the tower. $\bar{r}_x(x)$, $\bar{r}_y(x)$ and $\bar{r}_\theta(x)$ are the static displacements given by the mean wind velocity *V*(*x*), while $r_x(x,t)$, $r_y(x,t)$ and $r_\theta(x,t)$ are the additional fluctuating responses induced by turbulence. Wind velocity in the displaced configuration is $V + u(x,t)$ in the along-wind direction and $v(x,t)$ in the direction perpendicular to main flow.

According to Strømmen (2010), the forces on the structure in form of drag, lift and moment in the displaced position are defined by:

$$\begin{bmatrix} q_D(x,t) \\ q_L(x,t) \\ q_M(x,t) \end{bmatrix} = \frac{1}{2} \cdot \rho \cdot V_{rel}^2 \cdot \begin{bmatrix} D \cdot C_D(\alpha) \\ B \cdot C_L(\alpha) \\ B^2 \cdot C_M(\alpha) \end{bmatrix} \tag{11}$$

V_{rel} is the instantaneous relative velocity at height *x*, α is the angel of flow compared to the cross-sectional axis at the same instance. The *C*-factors are load coefficients. Using Fig. 1, these forces could be related to the structural coordinate system by:

$$\mathbf{q}_{tot}(x,t) = \begin{bmatrix} q_y \\ q_z \\ q_\theta \end{bmatrix}_{tot} = \begin{bmatrix} \cos\beta & -\text{sen}\beta & 0 \\ \text{sen}\beta & \cos\beta & 0 \\ 0 & 0 & 1 \end{bmatrix} \cdot \begin{bmatrix} q_D \\ q_L \\ q_M \end{bmatrix} \tag{12}$$

The β -angle could be found from the Fig. 1 as $\beta = \arctan\left(\frac{v-\dot{r}_z}{V+u-\dot{r}_y}\right)$. It is now assumed that the turbulence components *u* and *v* are small compared to the mean wind velocity *V*, and that the cross-sectional displacements r_i $(i = y, z, q)$ are small. Using these assumptions it could easily be shown that the following linearization applies.

$$\begin{aligned} &\mathrm{V}_{rel}^2 \approx \mathrm{V}^2 + 2Vu - 2V\dot{r}_y \\ &\alpha \approx \bar{r}_\theta + r_\theta + \frac{v}{V} - \frac{\dot{r}_z}{V} \end{aligned} \tag{13}$$

Still according to Strømmen (2010), the drag, lift and moment coefficients from Eq. (11) depend nonlinearly on the angle α. Considering α as two parts $\bar{\alpha} = \bar{r}_\theta$ and $\bar{\alpha}_f = r_\theta + v/V - \dot{r}_z/V$ induced by the mean wind velocity and the fluctuations respectively, the load coefficients *C* could be separately divided.

$$\begin{bmatrix} C_D(\alpha) \\ C_L(\alpha) \\ C_M(\alpha) \end{bmatrix} = \begin{bmatrix} C_D(\bar{\alpha}) \\ C_L(\bar{\alpha}) \\ C_M(\bar{\alpha}) \end{bmatrix} + \alpha_f \begin{bmatrix} C_D'(\bar{\alpha}) \\ C_L'(\bar{\alpha}) \\ C_M'(\bar{\alpha}) \end{bmatrix} \tag{14}$$

Combining Eqs. (11) to (14), discarding higher order terms (i.e. terms containing the product of quantities that have been assumed small) and focusing on the y-direction only the following is obtained:

$$q_{y,tot}(x,t) = \bar{q}_y(x) + q_y(x,t) = \bar{q}_y + \mathbf{B}_{q,y} \cdot \mathbf{v} + \mathbf{C}_{ae,y} \cdot \dot{\mathbf{r}} + \mathbf{K}_{ae,y} \cdot \mathbf{r} \tag{15}$$

where

$$\mathbf{v}(x,t) = \begin{bmatrix} u & v \end{bmatrix}^T \tag{16}$$

$$\mathbf{r}(x,t) = \begin{bmatrix} r_y & r_z & r_\theta \end{bmatrix}^T \tag{17}$$

$$\bar{q}_y = \frac{\rho V(x)^2}{2} \cdot \left(\frac{D}{B}\right) \bar{C}_D \tag{18}$$

$$\mathbf{B}_{q,y}(x) = \frac{\rho V(x) B}{2} \begin{bmatrix} 2\frac{D}{C}\bar{C}_D & \left(\frac{D}{B}\right)C_D' - \bar{C}_L \end{bmatrix} \tag{19}$$

$$\mathbf{C}_{ae,y} = -\frac{\rho V(x) B}{2} \begin{bmatrix} 2\frac{D}{C}\bar{C}_D & \left(\frac{D}{B}\right)\cdot C_D' - \bar{C}_L & 0 \end{bmatrix} \tag{20}$$

$$\mathbf{K}_{ae,y} = \frac{\rho V(x)^2 B}{2} \begin{bmatrix} 0 & 0 & \frac{D}{C}\bar{C}_D \end{bmatrix} \tag{21}$$

2.3 Aerodynamics Derivatives

A further look at the aerodynamic properties should be included. $\mathbf{C}_{ae,y}$ and $\mathbf{K}_{ae,y}$ could be normalized and expressed by aerodynamic derivatives. For the y-direction properties this would, according to Strømmen, give:

$$\mathbf{C}_{ae,y} = \frac{\rho B^2}{2}\omega_i(V) \cdot \hat{\mathbf{C}}_{ae,y} = \frac{\rho B^2}{2}\omega_i(V) \begin{bmatrix} P_1^* & P_5^* & BP_2^* \end{bmatrix} \tag{22}$$

The non-dimensional P-factors are called aerodynamic derivatives. They could be determined by looking at Eq. (20).

$$\begin{bmatrix} P_1^* & P_5^* & BP_2^* \end{bmatrix} = \begin{bmatrix} -2\bar{C}_D \frac{D}{B}\frac{V(x)}{B\omega_i(V)} & -\left(\frac{D}{B}\bar{C}_D - \bar{C}_L\right)\left(\frac{V(x)}{B\omega_i(V)}\right) & 0 \end{bmatrix} \tag{23}$$

A similar expression as Eq. (22) could be established for $\mathbf{K}_{ae,y}$, but then normalized by $[\omega_i(V)]^2$. The term $[\omega_i(V)]^2$ is not cancelled out by the P*-factors, which results in a demand for iteration if $\mathbf{K}_{ae,y}$ should be included in the calculations. This is relevant for mean wind velocities approaching instability limits, which is not the case here. Therefore, $\mathbf{C}_{ae,y}$ contains all the relevant derivatives in this case.

From Eq. (15) the modal load is obtained by multiplying by the y-direction modal vector.

$$\tilde{Q}_{y,tot}(t) = \int_{L_{\text{exp}}} \phi_y(x) \cdot q_{y,tot}(x,t) dx \tag{24}$$

The total load $q_{y,tot}(x,t)$ could by Eq. (15) be separated into a flow induced and an aerodynamic part, like shown for the modal load in Eq. (1). All aerodynamic properties are moved to the left hand side of the equation. system, and included in the frequency response function $\hat{H}(\omega)$. With the aerodynamic properties out of the picture, the load terms left are:

$$q_{y,tot}(x,t) = \bar{q}_y(x) + \mathbf{B_q} \cdot \mathbf{v}(x,t) \tag{25}$$

Only the flow induced contribution $\mathbf{B_q} \cdot \mathbf{v}$ will be considered in the following, while the static loading $\bar{q}_y$ has been assessed in Section 6.2.1. Combining Eqs. (16), (19) and (24), the modal loading induced by flow is:

$$Q_y(t) = \frac{\rho V(x) B}{2} \int_{L_{\text{exp}}} \phi_y(x) \cdot \left[\frac{2D\bar{C}_D}{B} \cdot u(x,t) + \left(\frac{DC'_D}{B} - \bar{C}_L \right) \cdot v(x,t) \right] dx \tag{26}$$

Fourier transform of Eq. (26) gives:

$$a_{\tilde{Q}_y}(\omega) = \frac{\rho V(x) B}{2} \int_{L_{\text{exp}}} \phi_y(x) \cdot \left[\frac{2D\bar{C}_D}{B} \cdot a_u(x,\omega) + \left(\frac{DC'_D}{B} - \bar{C}_L \right) a_v(x,t) \right] dx \tag{27}$$

The spectral density of loading is then given by:

$$\begin{aligned} S_{\tilde{Q}_y}(\omega) = \lim_{T\to\infty} \frac{1}{\pi T} \cdot a^*_{\tilde{Q}_y} \cdot a_{\tilde{Q}_y} = \left(\frac{\rho V(x) B}{2} \right)^2 \lim_{T\to\infty} \frac{1}{\pi T} \cdot \left\{ \int_{L_{\text{exp}}} \phi_y(x) \cdot \left[\frac{2D\bar{C}_D}{B} \cdot a^*_u(x,\omega) + \left(\frac{DC'_D}{B} - \bar{C}_L \right) a^*_v(x,t) \right] dx \right\} \\ \cdot \left\{ \int_{L_{\text{exp}}} \phi_y(x) \cdot \left[\frac{2D\bar{C}_D}{B} \cdot a_u(x,\omega) + \left(\frac{DC'_D}{B} - \bar{C}_L \right) a_v(x,t) \right] dx \right\} \end{aligned} \tag{28}$$

2.4 Joint Acceptance Function (JAF)

The load spectral density from Eq. (28) contains cross spectral densities between turbulence components *u* and *v*. These cross spectral densities are usually small, and are therefore neglected. Rewriting Eq. (28) gives:

$$S_{\tilde{Q}_y}(\omega) = \iint_{L_{\text{exp}}} \phi_y(x_1) \cdot \phi_y(x_2) \cdot \left(\frac{\rho V(x) B}{2} \right)^2 \cdot \left\{ \begin{aligned} &\left[\left(\frac{2D\bar{C}_D}{B} \right)^2 \cdot \lim_{T\to\infty} \frac{1}{\pi T} \cdot a^*_u(x_1,\omega) \cdot a_u(x_2,\omega) \right] \\ &+ \left[\left(\frac{DC'_D}{B} - \bar{C}_L \right)^2 \cdot \lim_{T\to\infty} \frac{1}{\pi T} \cdot a^*_v(x_1,\omega) \cdot a_v(x_2,\omega) \right] \end{aligned} \right\} dx_1 dx_2 \tag{29}$$

The introduction of integration variables x_1 and x_2 is necessary to transform the integral product from Eq. (28) into a double integral. To proceed the following definitions are introduced:

$$S_{nn}(\Delta x,\omega) = \lim_{T\to\infty} \frac{1}{\pi T} \cdot \left[a^*_n(x_1,\omega) \cdot a_n(x_2,\omega) \right];\ I_n(x) = \frac{\sigma_n(x)}{V(x)} \tag{30}$$

$I_n(z)$ is the turbulence intensity, while $S_{nn}(x)$ is the cross spectral density. The turbulence intensity is equal to the ratio between standard deviation of the turbulent component and the mean wind velocity. According to Strømmen (2010), the turbulence intensity perpendicular to main flow is equal to 3/4 of the turbulence intensity in the main flow direction. Using Eq. (30) and expanding Eq. (29), it is obtained from Eq. (29) that:

$$S_{\bar{Q}_y}(\omega) = \left[\frac{\rho B}{2} \cdot J_y(\omega)\right]^2 \tag{31}$$

Where the joint acceptance function $J_y(\omega)$ is given by:

$$J_y^2(\omega) = \iint_{L_{exp}} \phi_y(x_1) \cdot \phi_y(x_2) \cdot \left(V(x_1)^2 \cdot V(x_2)^2\right) \left\{ A(x_1) \cdot A(x_2) \cdot \frac{S_{uu}(\Delta x, \omega)}{\sigma_u^2} + B(x_1) \cdot B(x_2) \cdot \frac{S_{vv}(\Delta x, \omega)}{\sigma_v^2} \right\} dx_1 dx_2 \tag{32}$$

where

$$A(x_i) = \left(\frac{2D\bar{C}_D}{B} I_u(x_i)\right), \ \mathrm{B}(x_i) = \left(\left(\frac{DC'_D}{B} - \bar{C}_L\right) I_v(x_i)\right), \ i = 1,2 \tag{33}$$

The JAF describes how the structural mode shapes interact with the loading (and therefore the frequency and spatial properties of the air flow). It should be mentioned that the function calculated is not actually the JAF. For practical reasons, the wind velocity is included in the integral. This is not done in the JAF shown by Strømmen (2010) because the wind velocity is constant for bridge decks at constant heights. For the given case however, the wind velocity varies over the height of the structure. Including the velocity terms in the JAF is both convenient and saves computation time.

The cross spectral density functions $S_{nn}(\Delta x, \omega)$ describes the density of fluctuations in the n-direction with a given frequency for two points located a distance $\Delta x = |x_1 - x_2|$ from each other. It could, by using the definition of Co-spectrums, be written as the product of the normalized Co-spectrum and the spectral density of the relevant turbulence component, i.e.

$$\frac{S_{nn}(\Delta x, \omega)}{\sigma_n^2} = \frac{S_n(\omega)}{\sigma_n^2} \cdot \hat{Co}_{nn}(\Delta x, \omega) \tag{34}$$

The spectral density $S_n(\omega)/\sigma_n^2$ is a probabilistic way of describing the amount of turbulence fluctuations over the frequency spectrum. In other words, it describes if turbulence fluctuations of a given frequency are common or not. Kaimal et al. (1972) proposed an expression that has been frequently used, and has been adopted by the Eurocode (2010). Looking to Dyrbye and Hansen (1999), the following version of the Kaimal spectral density is given:

$$\frac{S_n(\omega)}{\sigma_n^2} = \frac{6{,}8 f_L}{\omega(1+10{,}2 f_L)^{5/3}} \tag{35}$$

The term f_L is given by $f_L = \dfrac{\omega \cdot {}^{s}L_n}{2\pi \cdot V(x)}$. ${}^{s}L_n$ is an integral length scale, and could according to Dyrbye and Hansen (1999) be interpreted as the average size of a gust in a given direction *s*. For a tower structure, the relevant direction is the same as the main flow, which here is denoted as *y*. The two considered turbulence components are *u* and *v*. Strømmen (2010) states that these eddy sizes should be obtained from full scale measurements. As an approximation, the following could be adopted:

$${}^{y}L_u = 100 \cdot \left(\frac{x_f}{10}\right)^{0,3}, \ {}^{y}L_v = \frac{{}^{y}L_u}{4}, \begin{cases} x_f = 10 \text{ for } x \le 10 \text{ m} \\ x_f = x \text{ for } x > 10 \text{ m} \end{cases} \tag{36}$$

Normalized Co-spectrums represent the spatial properties of the wind turbulence, and are often encountered in literature. As shown in Eq. (34), $\hat{Co}$ depends on the spacing between two considered points, Δx. If two points are located far from each other, the wind fields experienced at the two points could not be expected equal, and thus the cross spectral density is scaled down by $\hat{Co}_{nn}$. If the two points are closely spaced, they will experience similar wind fields, and thus the cross spectral density will not be reduced.

One of the most commonly used expressions for $\hat{Co}_{nn}$ was developed by Davenport (1962). Using empirical results from line like structures in flat terrain, the following expression was established for the Co-spectrum

$$\hat{Co}_{nn}(\Delta x,\omega)=e^{-C_{nm}\frac{\Delta x\cdot\omega}{2\pi\cdot\bar{V}(x)}},n=u,v\ ;m=x,y,z \tag{37}$$

C_{mn} is a decay constant that describes the spatial extent of turbulence correlation. It was conservatively estimated by Davenport (1962) to the value C_{uz} = 7 . This value displays great variations. Dyrbye and Hansen (1999) suggests C_{uz} = 10, while Strømmen (2010) suggests $C_{uz} \approx 9$. The latter value is adopted in this research.

2.5 Standart Deviation of Buffeting Response

The standard deviation of displacement is found by integrating the displacement response spectrum over the entire frequency domain.

$$\sigma_{r_y}^2(x)=\int_0^\infty S_{r_y}(x,\omega)d\omega \tag{38}$$

The acceleration is usually found as the displacement derived twice with respect to time. The spectral density of acceleration is given by:

$$\sigma_{a_n}^2=\int_0^\infty S_{a_n}(\omega)d\omega=\omega_n^4\cdot\int_0^\infty S_{r_n}(\omega)d\omega \tag{39}$$

3. BENCHMARK MODEL

In this study, the model has 20 floors, in which the height of each level was 3.0 m. Floor plan and its dimensions are illustrated in Fig. 2. Lateral resisting system in Model A is a two-cell semi-open core, and its details are illustrated in section B–B in Fig. 2. All calculations were performed as linear static and dynamic analysis using SAP2000 software.

Some simplifications were considered in modeling of buildings: (a) the floor slab is assumed to act as absolutely rigid diaphragms (no in-plan deformation); (b) flexural as well as axial, shear and torsion deformation in horizontal elements has not been taken into account; and (c) small eccentricities in the connections of beams and columns were neglected.

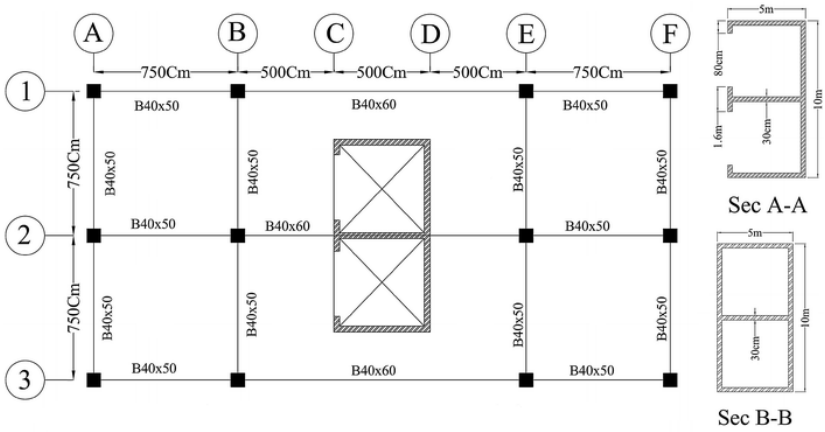

Figure 2. Floor plan and core wall section dimensions.

3.1 Natural frequencies and modal shapes

The results of the model in SAP2000 showed that mode 1 contains modal displacement in the longitudinal direction of the structure. The second mode contains modal displacement in the transverse direction, while the third mode is a torsional mode. The three modal shapes can be seen in Fig. 3 and their natural frequency values are show in Tab. 1. As it can see in Tab. 1, the first two modes have significant periods when compared to the third mode.

Table 1. Natural frequencies and periods, modes 1 to 3.

Mode #	Frequency [Hz]	Angular frequency [rad/s]	Period [s]
1	0,7718	4,8496	1,296
2	0,924	5,806	1,082
3	1,155	7,263	0,865

From Fig. 3 it can be seen that the structure has a behavior similar of the cantilever beam where the first mode has modal displacements in the longitudinal direction and the second mode has modal displacements in the transverse direction. The core section is arranged to provide large stiffness to the structure in the transverse direction.

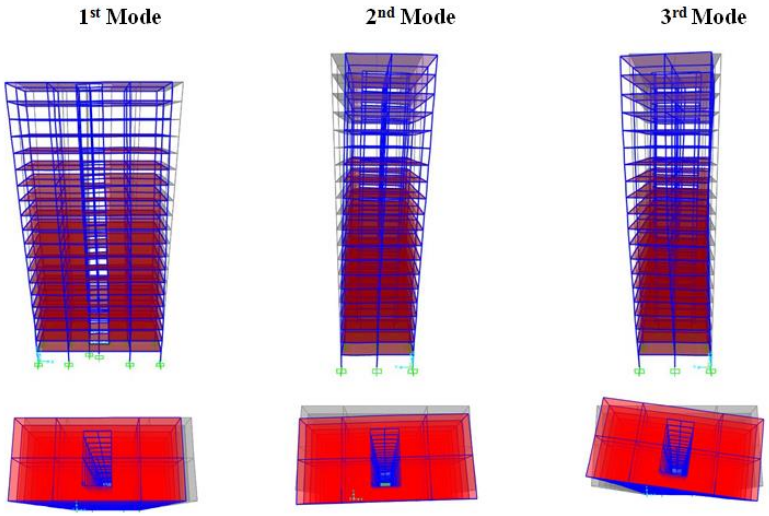

Figure 3. Modal shapes of the structure.

Modal shapes could be represented more exact by the displacements at each floor. For simplicity, a node at one corner of each floor has been chosen to represent the displacements. Figure 4 presents the shapes of mode 1 and 2. It should be mentioned that the units of the displacement values are useless. Modal calculations are performed without loading, making the displacement values hard to interpret.

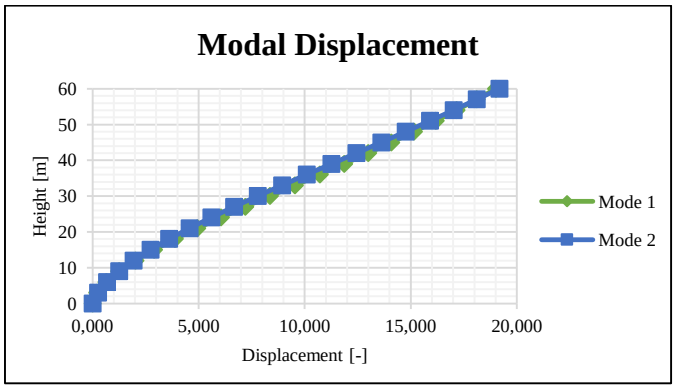

Figure 4. Modal displacements from SAP2000, modes 1 and 2.

4. SIMULATION RESULTS

MATLAB calculations have been performed using the theoretical basis presented in section 2. As mentioned earlier, single component response has been calculated for modes 1 and 2 separately.

Initially, the Kaimal spectral density is obtained. This quantity is a function of frequency, and it is calculated for both *u* and *v* turbulence. Figure 5 (a) shows the *u*-component Kaimal spectral density multiplied by the frequency of Mode 1.

It should be mentioned that the resolution of the ω-vector combined with the logarithmic plotting makes the function look linear for low values of ω. However, this has little effect for the calculations. It is seen that S_{ka} decreases for high frequencies. Physically, the figure illustrates the density of fluctuations of a given frequency. It is seen that wind fluctuations with a frequency between 0.02 and 2 rad/s are most frequently experienced.

As mentioned earlier, the wind velocity is included when the JAF is calculated. This results in values that are away higher than what could normally be expected for the JAF. Figure 5 (b) shows the JAF for modes 1 and 2.

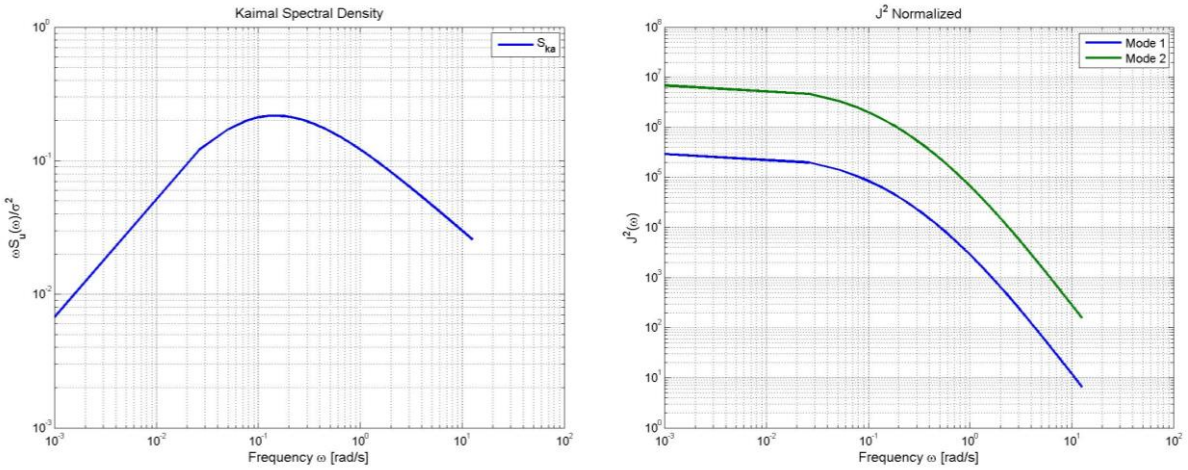

(a) **(b)**

Figure 5. (a) Kaimal spectral density, *u*-component; (b) Joint acceptance function, modes 1 and 2.

It is seen that the JAF has maximal values of about 10^5 for Mode 1, and 10^6 for Mode 2. The wind velocity is included in the JAF integral in the fourth power, and thus the contribution from V_m to the total JAF should approach 10^5. This argues that the value of the JAF is reasonable (between 0.1 and 10 for low frequencies). It is noted that the JAFs decrease for high frequency values.

In Strømmen (2010), Appendix B, joint acceptance functions for several shape functions have been plotted. The JAFs in this work correspond well to the JAF obtained by Strømmen for the shape $\phi = x$, which corresponds fairly well to the actual modal shapes of the structure. In other words, the JAFs resemble what could be expected for the given modal shapes.

Response Spectrums for acceleration and displacement are crucial in the calculations. To illustrate these quantities, they are shown for Mode 1 in Fig. 6. As expected, both response spectrums have clear peaks for the eigen frequency of Mode 1. It is seen that contributions to the acceleration from low frequencies are almost negligible, while low frequencies will contribute somewhat more to the displacement.

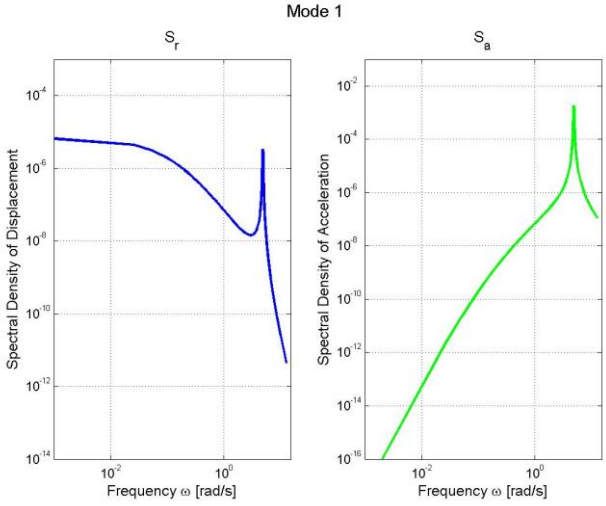

Figure 6. Spectral densities of displacement and acceleration, Mode 1.

As mentioned earlier, time series simulations of spectral densities could be obtained. Such simulations illustrate the structural motion, and indicates which values could be expected for dynamic displacements and accelerations. It is noted that results vary with the used phase angle, and thus plots will be different for every calculation (see Eq. (10)). Time domain plots for Mode 1 are shown in Fig. 7 (a). The considered time span is 10 minutes (600 s).

It is seen that the dynamic displacements have maximal values close to 4 mm. The acceleration seems to have maximal values of about 0.05 m/s^2. It seems as the acceleration comes in pulses, with peaks every 3-4 minutes. The time domain simulations for Mode 2 are shown in Fig. 7 (b).

Looking at Fig. 7 (b), it is seen that the dynamic displacements have maximal values of about 6 mm, the same as for Mode 1. The acceleration once again comes in pulses, but these are more closely spaced than what was observed for Mode 1. The maximal acceleration of Mode 2 seems to approach 0.1 m/s^2.

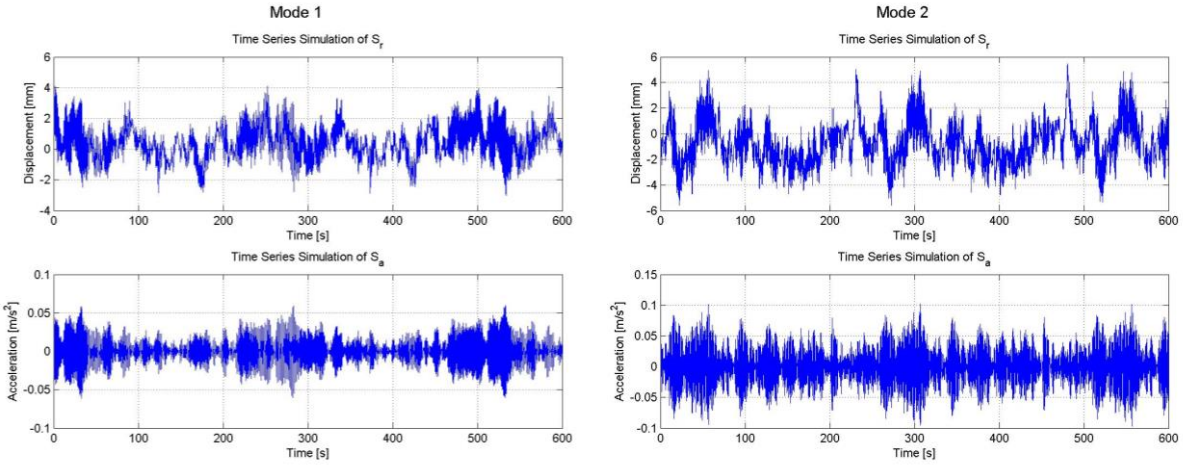

(a) **(b)**

Figure 7. Spectral densities and time domain simulation of displacement and acceleration, Modes 1 (a) and 2 (b).

5. CONCLUSIONS

A MATLAB script was made to perform calculations using given and estimated input values to fit displacements and accelerations for the two first translational modes. The script carried out time domain simulation for a single mode excitation of the structure after the calculation of their spectral densities. Response referred to as Mode 1 values describes results for wind loading against the short side of the building, which excites the first structural mode. Similarly, response and forces referred to as Mode 2 values describes results for wind loading against the long side of the building, which excites the second mode.

The maximal accelerations obtained from time simulations seems to approach to 0.05 m/s^2 in Mode 1, and 0.1 m/s^2 in Mode 2. It is seen that the JAFs correspond fairly well to the actual modal shapes of the benchmark structure. In other words, the JAFs resemble what could be expected for the given modal shapes.

6. REFERENCES

Braga, W.A., 2018. *Avaliação do comportamento dinâmico de edifícios com base em critérios de conforto humano*. BE-thesis, Universidade Federal do Ceará, Fortaleza, Brazil.

Davenport, A.G, 1962. "The Response of Slender, Line-Like Structures to a Gusty Wind". *Ice Proceedings*, Vol. 23, pp. 389–408.

Dyrbye, C. and Hansen, S.O., 1999. *Wind Loads on Structures*. Wiley, Chichester.

Kaimal, J.C., Wyngaard, J. C., Izumi, Y. and Coté, O. R., 1972. "Spectral characteristics of surface-layer turbulence". *Quarterly Journal of the Royal Meteorological Society*, Vol. 98, pp. 563–589.

Strømmen, E. N., 2010. *Theory of Bridge Aerodynamics*. Springer, Berlin, 2nd edition.

7. RESPONSIBILITY NOTICE

The authors are the only responsible for the printed material included in this paper.